Structural Trends in Divalent Benzil Bis(thiosemicarbazone) Complexes

David G. Calatayud,[a] Elena López-Torres,[a] M. Antonia Mendiola,*[a] César J. Pastor,[b] and Jesús R. Procopio[c]

Keywords: Copper / N ligands / S ligands / Thiosemicarbazone complexes / Zinc

Redox-related changes in the biological properties of copper bis(thiosemicarbazones) are induced by the backbone of the ligand. To get information about how these changes depend on the structural parameters, three X-ray structures of complexes with different behaviour of the benzil bis(thiosemicarbazone) ligand have been determined. These include two almost planar copper(II) complexes with different grades of deprotonation in the ligand and a Zn^{II} complex in which the ligand acts as a monoanion and a nitrate group is bonded to the metal ion in a square-based pyramid. The changes in the backbone bond lengths agree with the variation in the ionic radius and with the grade of electronic charge delocalisation in the chelate rings; these have consequences for the coordination sphere, allowing the metal to fit slightly better into the ligand cavity, which in turn may affect the complex stability and the redox potential.

Introduction

The increasing interest in thiosemicarbazones (TSCs) that has arisen in the last decades is related to their wide range of biological properties, for example as antiviral, antibacterial and anticancer agents.[1–4] These biological activities are often attributed to their chelating ability with metal ions. Copper complexes of bis(thiosemicarbazones) have been investigated for use as anti-cancer chemotherapeutic agents[5,6] and as superoxide dismutase-like radical scavengers.[7] It is, however, their use as delivery agents for radioactive copper in new copper-based radiopharmaceuticals and the hypoxic selectivity of certain copper bis(thiosemicarbazonate) complexes that has created much recent interest.[8–20] The biological characteristics of copper bis(thiosemicarbazonate) complexes derived from 1,2-diones are dependent on the nature of the "backbone" substituents in the ligand. The most detailed studies of these structure–activity relationship have been carried out in connection with hypoxia imaging.[14,15,21] These studies correlated hypoxic cell selectivity with the reduction potential, electronic structure and chemical behaviour and found that all of these properties are extraordinarily sensitive to the alkyl groups attached to the diimine backbone of the ligand. The trapping in a hypoxic cell is believed to occur by reduction of the copper(II) complex by intracellular reducing agents to give stable protonated Cu^{I} species, which are trapped inside the cell.[22] The structure–activity relationships of copper bis(thiosemicarbazone) radiopharmaceuticals derived from 1,2-diones show a correlation between the reduction potential for the Cu^{II}/Cu^{I} couple and the hypoxic cell selectivity.[14,23] The hypoxia-selective radiopharmaceutical [Cu(ATSM)] [ATSM = biacetyl bis(4-methylthiosemicarbazone)], for example, undergoes a reversible reduction at $E_{1/2}$ = –0.620 V in DMF at a glassy carbon working electrode. On the other hand, some zinc thiosemicarbazone complexes that have been shown to be active as anti-tumour agents are as cytotoxic as cisplatin and are also effective against cisplatin-resistant cell lines.[24] Recently, fluorescence studies and the cellular distribution of zinc bis(thiosemicarbazone) complexes have been reported.[25]

Since relatively superficial modifications induce remarkable changes in redox and biological properties, it is natural to enquire whether they might also significantly affect the core structural parameters of the complexes and, if so, whether this might be related to their biological behaviour. The aim of this work is to get information about the importance of the changes induced by the modification of the backbone of benzil bis(thiosemicarbazone) (LH_6) in some complexes. In particular, for copper(II) complexes these changes affect the redox properties and therefore their potential activity as hypoxia-selective radiopharmaceuticals. We report the X-ray structures of two copper complexes derived from LH_6 (Figure 1) whose reduction potential values are –0.550 and –0.520 V,[26] close to those of [Cu(ATSM)], a related zinc complex, as well as the structure of a nickel complex for comparison.[27] We also discuss structural variations as a function of the ligand behaviour and/or the metal ion.

[a] Departamento de Química Inorgánica, Universidad Autónoma, 28049 Madrid, Spain
E-mail: antonia.mendiola@uam.es
[b] Servicio Interdepartamental de Investigación, Universidad Autónoma, 28049 Madrid, Spain
[c] Departamento de Química Analítica y Análisis Instrumental, Universidad Autónoma, 28049 Madrid, Spain

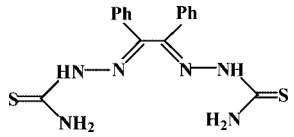

Figure 1. Drawing of benzil bis(thiosemicarbazone) (LH_6).

Results

All complexes were synthesised as described previously, except complex **2**, which was isolated from the mother liquor of the synthesis of a previously published complex.[26] Their analytical and spectroscopic properties are consistent with those reported previously.[26,28] Complex **2** presents a 1:1 ligand:copper molar ratio and has a nitrate group as a counterion.

In complex **1**, which was prepared from copper(II) chloride, benzil bis(thiosemicarbazone) acts as a dianion, while in complexes **2** and **3**, which were synthesised from copper and zinc nitrate, respectively, it has lost only a hydrazinic hydrogen atom and therefore acts as a monoanion. However, the nitrate ion contained in **2** and **3** shows a different behaviour: it is outside of the coordination sphere in the first complex but is bonded to the zinc atom in complex **3**.

The crystal structures of all complexes consist of discrete molecules where the ligand is tetradentate through the imine nitrogen and the sulfur atoms by changing the *trans* disposition of the thiosemicarbazone moieties in the free ligand to *cis* to form an N_2S_2 chelate, as has been observed in other complexes.[27]

The crystal structure of **1** consists of discrete molecules of [$CuLH_4$]. A perspective view of the complex, together with the atom-labelling scheme, is given in Figure 2 (the thermal ellipsoids are shown at 50% probability) and selected bond lengths and angles are given in Tables 1 and 2, respectively. The crystallographic data of the complex confirm the geometry proposed from spectroscopic data[26] and the cell parameters are close to those reported previously.[29] The copper(II) ion is tetracoordinate in a planar disposition. The coordination sphere of the copper atom is formed by two sulfurs and two imine nitrogens, as expected for this ligand.[30,31] The environment of the copper ion is planar, with a distance from the copper ion to the basal plane of 0.1219 Å. The phenyl rings C(5)–C(10) and C(11)–C(16) form dihedral angles of 81.9° and 81.0°, respectively, with respect to the basal plane. The molecules are held together in the crystal packing through an extended network of intermolecular hydrogen bonds involving the amino groups and the hydrazinic nitrogen atoms (see Figure 3 and Table 3).

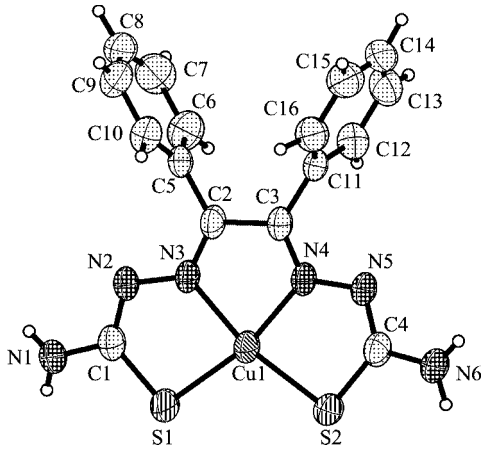

Figure 2. XSHELL view of [$CuLH_4$] (**1**).

The structure determination of [$CuLH_5$]NO_3 (**2**; Figure 4 with the thermal ellipsoids shown at 50% probability. See also Tables 1 and 2) shows a similar disposition for the copper ion as in complex **1**, but with a nitrate group acting as a counterion, although a weak interaction with the copper ion is also observed [*d*(Cu–O) = 2.46 Å]. The bis(thiosemicarbazone) acts as an N_2S_2 chelate ligand around the metal ion, giving a quasi-planar geometry for the copper with a deviation of 0.2084 Å from the basal plane. The main difference is the unusual asymmetric behaviour of the thiosemi-

Table 1. Selected bond lengths [Å] for the complexes and ligand LH_6.

	1	**2**	**3**	**4**[27]	LH_6[27]
C(2)–C(3)	1.485(3)	1.481(3)	1.491(3)	1.475(3)	1.478(3)
C(2)–C(5)	1.484(3)	1.480(3)	1.483(3)	1.474(3)	1.490(3)
C(3)–C(11)	1.482(3)	1.478(3)	1.490(3)	1.474(3)	1.490(3)
C(2)–N(3)	1.293(3)	1.305(3)	1.300(3)	1.308(3)	1.298(3)
C(3)–N(4)	1.296(3)	1.295(3)	1.285(3)	1.307(3)	1.294(3)
N(3)–N(2)	1.357(3)	1.351(2)	1.357(2)	1.372(3)	1.361(3)
N(4)–N(5)	1.363(3)	1.361(2)	1.357(3)	1.371(3)	1.362(3)
N(2)–C(1)	1.324(3)	1.333(3)	1.341(3)	1.329(3)	1.369(3)
N(5)–C(4)	1.327(3)	1.356(3)	1.352(3)	1.320(3)	1.367(3)
C(1)–S(1)	1.754(3)	1.751(2)	1.739(2)	1.745(3)	1.667(3)
C(4)–S(2)	1.744(3)	1.712(2)	1.707(2)	1.744(3)	1.668(3)
N(3)–M	1.976(2)	1.9873(17)	2.1407(19)	1.861(2)	
N(4)–M	1.968(2)	1.9682(17)	2.1290(18)	1.862(2)	
S(1)–M	2.2356(8)	2.2458(5)	2.3143(6)	2.1572(7)	
S(2)–M	2.2332(8)	2.2844(6)	2.3695(7)	2.1461(7)	
C(1)–N(1)	1.322(4)	1.329(3)	1.338(3)	1.330(3)	1.305(3)
C(4)–N(6)	1.334(4)	1.314(3)	1.319(3)	1.342(3)	1.306(4)
O(1)–M			2.1142(17)		

Table 2. Bond angles [°] for the complexes and ligand LH_6.

	1	**2**	**3**	**4**[27]	LH_6[27]
N(3)–C(2)–C(3)	114.4(2)	114.13(18)	114.1(2)	111.8(2)	114.0(2)
N(4)–C(3)–C(2)	114.7(2)	113.90(18)	114.35(19)	113.1(2)	114.2(2)
C(2)–N(3)–M	114.50(16)	115.40(14)	117.66(15)	116.09(16)	
C(3)–N(4)–M	114.54(16)	116.64(14)	118.88(14)	115.41(17)	
N(2)–N(3)–M	123.05(16)	122.74(13)	121.04(14)	123.43(15)	
N(5)–N(4)–M	123.22(17)	119.56(13)	118.16(14)	123.89(16)	
N(3)–N(2)–C(1)	111.6(2)	111.75(16)	111.65(18)	110.1(2)	119.0(2)
N(4)–N(5)–C(4)	110.8(2)	116.89(17)	118.26(19)	109.5(2)	119.1(2)
N(2)–C(1)–S(1)	125.6(2)	125.80(16)	128.33(17)	124.41(19)	118.68(19)
N(5)–C(4)–S(2)	126.4(2)	122.09(16)	123.20(17)	124.81(19)	118.3(2)
C(1)–S(1)–M	94.71(9)	94.55(7)	95.68(8)	94.11(8)	
C(4)–S(2)–M	94.49(9)	95.76(7)	97.24(8)	94.26(8)	
N(3)–M–N(4)	81.06(8)	79.87(7)	73.46(7)	83.32(8)	
N(3)–M–S(1)	84.96(6)	84.89(5)	81.93(5)	87.62(6)	
N(4)–M–S(2)	85.09(6)	85.33(5)	81.37(5)	87.38(7)	
S(1)–M–S(2)	108.80(3)	108.52(2)	115.57(2)	101.69(3)	
N(3)–M–S(2)	165.73(6)	161.90(5)	147.35(5)	170.68(6)	
N(4)–M–S(1)	165.98(7)	163.79(5)	152.24(6)	170.87(7)	
C(2)–N(3)–N(2)	122.2(2)	121.83(17)	120.48(19)	120.5(2)	118.7(2)
C(3)–N(4)–N(5)	122.2(2)	123.65(17)	122.96(18)	120.7(2)	118.9(2)
C(5)–C(2)–C(3)	120.6(2)	121.15(18)	120.24(19)	123.2(2)	121.0(2)
C(11)–C(3)–C(2)	121.3(2)	121.91(18)	121.45(19)	122.7(2)	120.2(2)
C(5)–C(2)–N(3)	125.0(2)	124.72(18)	125.64(19)	125.0(2)	125.0(2)
C(11)–C(3)–N(4)	124.0(2)	124.13(18)	124.2(2)	124.1(2)	125.6(2)
N(2)–C(1)–N(1)	117.9(3)	116.93(19)	115.7(2)	117.3(2)	115.8(2)
N(5)–C(4)–N(6)	116.8(3)	115.9(2)	115.9(2)	117.9(2)	115.7(3)
N(1)–C(1)–S(1)	116.5(2)	117.26(16)	115.99(18)	118.3(2)	125.6(2)
N(6)–C(4)–S(2)	116.9(2)	122.00(17)	120.92(19)	117.3(2)	126.0(2)

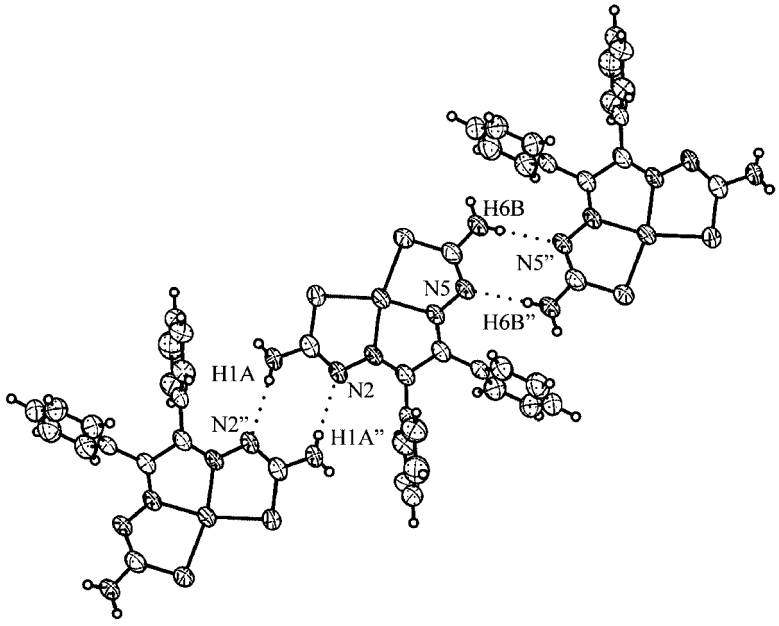

Figure 3. Plot of complex $[CuLH_4]$ (**1**) showing the hydrogen bonds.

carbazone branches of the ligand, due to the presence of the hydrogen atom in a secondary amine for only one thiosemicarbazone moiety. The phenyl rings C(5)–C(10) and C(11)–C(16) form dihedral angles of 65.0° and 58.3°, respectively, with respect to the basal plane. The presence of an additional hydrogen together with the nitrate group allows this complex to form additional hydrogen bonds, as shown in Figure 5 and Table 3.

Yellow crystals of complex **3** were obtained by recrystallisation from methanol. Discrete $[ZnLH_5NO_3]$ entities form

Table 3. Hydrogen bonds for complexes [Å and °].

	Interaction	*d*(D–H)	*d*(H···A)	*d*(D···A)	<(DHA)
1[a]	N(6)–H(6B)···N(5)#1	0.79(3)	2.28(3)	3.066(4)	176(3)
	N(1)–H(1A)···N(2)#2	0.76(4)	2.28(4)	3.030(4)	174(3)
2[b]	N(6)–H(6A)···O(3)#2	0.87(3)	2.03(3)	2.901(3)	179(3)
	N(5)–H(5···O(2)#2	0.82(3)	2.20(3)	2.932(2)	150(3)
	N(1)–H(1B)···N(2)#3	0.83(3)	2.18(3)	2.999(3)	176(3)
3[c]	N(1)–H(1B)···N(2)#1	0.74(3)	2.29(3)	3.023(3)	172(3)
	N(6)–H(6A)···O(2)#2	0.86(3)	2.10(3)	2.944(3)	169(3)
	N(6)–H(6B)···O(1)#3	0.84(39)	2.47(3)	3.153(3)	139(2)
	N(5)–H(5)···O(3)#2	0.82(39)	2.42(3)	3.062(3)	136(2)

[a] Symmetry transformations used to generate equivalent atoms: #1 $-x$, $-y$, $-z$; #2 $-x+2$, $-y$, $-z+1$. [b] Symmetry transformations used to generate equivalent atoms: #2 $-x+1$, $-y+1$, $-z$; #3 $-x+2$, $-y+2$, $-z+1$. [c] Symmetry transformations used to generate equivalent atoms: #1 $-x+2$, $-y+1$, $-z+1$; #2 $-x+1$, $-y+1$, $-z$; #3 $x-1$, y, z.

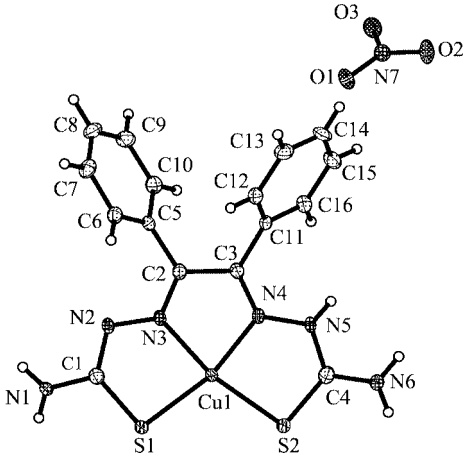

Figure 4. XSHELL view of $[CuLH_5]NO_3$ (**2**).

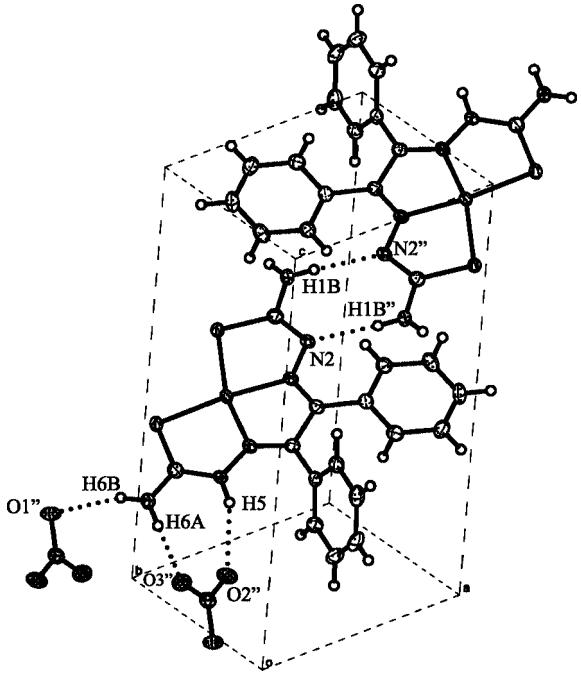

Figure 5. Plot of complex $[CuLH_5]NO_3$ (**2**) showing the hydrogen bonds.

the crystal structure of the complex (Figure 6 with the thermal ellipsoids shown at 50% probability. See also Tables 1 and 2). The benzil bis(thiosemicarbazone) acts as a monodeprotonated N_2S_2 ligand in a pseudo-planar disposition. The coordination sphere of the zinc atom is completed by an oxygen atom provided by the nitrate group to give a distorted square-based pyramidal geometry for the metal ion, as proposed from the spectroscopic data.[28] The value of the parameter, τ, defined by Addison et al.,[30] is 0.08 (τ = 0.0 for a regular square-based pyramid). The zinc atom is displaced by 0.439 Å out of the basal plane toward the oxygen atom at the apex of the pyramid. The phenyl rings C(5)–C(10) and C(11)–C(16) form dihedral angles of 63.6° and 57.0°, respectively, with respect to the basal plane. The molecules are bonded through hydrogen bonds between the amine and the nitrate groups (Figure 7, Table 3).

Discussion

The overall impression from the bonds and angles around the copper atoms (Tables 1 and 2) is that the ligand cavity is too small to accommodate the copper(II) ideally. The N–Cu–N bond angles are only 81.06° and 79.87° and the sulfur ends of the ligand arms are pushed outward well beyond the natural position that would be adopted by the planar ligand with 120° bond angles. For comparison, the Ni^{II} complex with the same ligand shows a much better fit[27] as a result of the smaller ionic radius of nickel, with Ni–N and Ni–S distances of 1.86 and 2.157 Å, respectively, compared to 1.976 Å (N) and 2.235 Å (S) and 1.987 Å (N) and 2.24 Å (S) for complexes **1** and **2**, respectively. All the angles at the nickel centre are significantly closer to the 90° preferred at the square-planar metal centre. Thus, the average N–Cu–N angle in our complexes is 80.45°, whereas for the nickel complex it is 83.32°. Similarly, the S–M–S angles are 108.7° for copper but only 101.68° for nickel, while the N–M–S angles are 85.21° for the copper complexes and 87.62° for the nickel complex.

Although the ligand appears somewhat strained in the copper complexes, it has been shown that the ligand can open up even further to accommodate Cd^{II} in its neutral form, while still maintaining an essentially planar structure.[28] As a result of the larger ionic radius of the zinc (giving two Zn–N distances of 2.1407 and 2.1290 Å and two Zn–S distances of 2.3143 and 2.3695 Å), all the angles are significantly far from 90°. Thus, the N–Zn–N angle is 73.46°, the S–Zn–S angle is 115.57° and the N–Zn–S angles are 81.93° and 81.37°. For comparison with the copper and nickel complexes, these data agree with the variation in the ionic radius for these ions even though the grade of deprotonation of the benzil bis(thiosemicarbazone) changes.

The backbone C(2)–C(3) distances in the complexes, except for the nickel complex, are larger than in the free ligand, ranging from 1.475 to 1.491 Å, in accordance with the metal ratio variations. The C(2)–N(3) distances range from 1.285 to 1.308 Å, and are consistent with a bond order greater than 1.5 but less than 2. The C(3)–N(4) bonds in

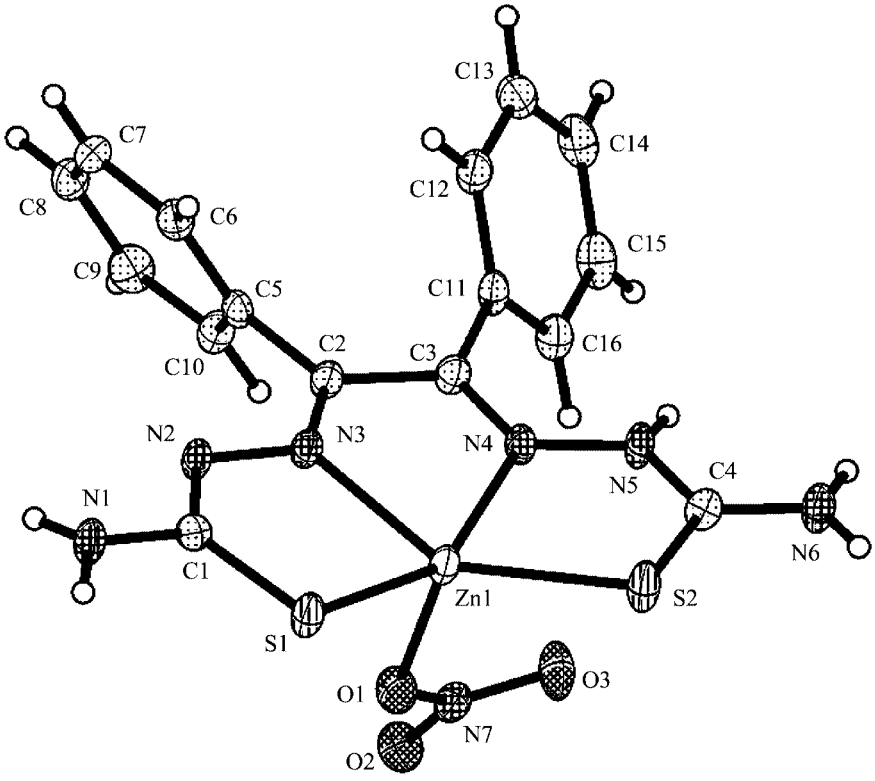

Figure 6. XSHELL view of $[ZnLH_5NO_3]$ (**3**).

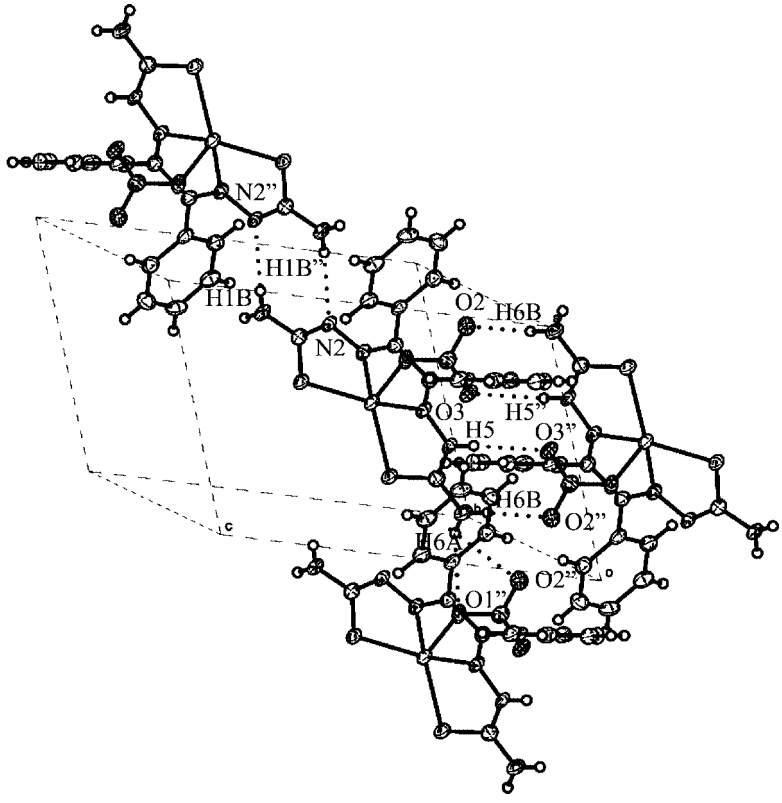

Figure 7. Plot of complex $[ZnLH_5NO_3]$ (**3**) showing the hydrogen bonds.

the non-deprotonated thiosemicarbazone branch are closer to a full double bond than in the deprotonated one. The N(2)–N(3) distances, which range from 1.351 to 1.371 Å, are consistent with a bond order less than 1.5 but greater than 1. The N(2)–C(1) distances are larger than the C(2)–N(3) distances, but are still greater than 1, and the N(5)–C(4) distances are larger than before, but shorter than in the free ligand. The C(1)–S(1) distances in the deprotonated thiosemicarbazone branch are much larger than in the non-deprotonated one [C(4)–S(2)] and are consistent with a bond order close to 1. The largest difference (0.084 Å) appears between the free ligand (1.667 Å) and complex **2** (1.751 Å). The C(1)–N(1) distances range from 1.328 to 1.338 Å and the C(4)–N(6) distances from 1.314 to 1.319 Å; they are intermediate between the C–N and N–CS distances. These data confirm there is extensive conjugation within the ligand that is greater in the deprotonated thiosemicarbazone branch.

The study of the electrochemical behaviour of the copper complexes was carried out in the range from +1 to –1.5 V.[26] In the positive range (+1 to 0 V), a quasi-reversible Cu^{III}/Cu^{II} oxidation process can be observed. Cyclic scanning between 0 and –1.5 V permits the study of the copper-centred reduction processes and the ligand reductions; the values of the potential for the Cu^{II}/Cu^{I} reduction processes are related to the biological activity. The cyclic voltammogram of complex **1** in the latter range shows a peak at –0.520 V in the cathodic scan, which can be attributed to the Cu^{II}/Cu^{I} reduction. Under the same conditions, the cyclic voltammogram of complex **2** shows waves at –0.600 V and –0.500 V associated with a quasi-reversible Cu^{II}/Cu^{I} process.

It appears that a relationship exists between the backbone C(2)–C(3) bond length and the categorisation according to reduction potential, and, in turn, with the biological behaviour, although any relationship between these structural parameters and biological function remains speculative. Thus, complex **1**, with a longer C(2)–C(3) bond than complex **2**, has a lower reduction potential (harder to reduce). As was mentioned in the introduction, the hypoxia selectivity (HSI) is related to the electrochemical behaviour, and those complexes with an HIS greater than 0.4 have a low redox reduction potential (<0.58 V).[14] Therefore, some hypoxic selectivity of complex **1**, which has a reduction potential of –0.550 V vs. Ag/AgCl, could be expected.

The ease of deformation away from planarity could be connected to the redox potential and other aspects of the redox behaviour because distorting ions towards tetrahedral favours the copper reduction and decreases the stability of the copper(II) complex. Complex **2** shows a slightly larger distance to the plane formed by the ligand than complex **1**, which agrees with the values of the reduction potential.[26] The grade of the deviation from planarity can be determined from the least-squares displacement of the ligand atoms from the mean plane of the complex. Figure 8 shows the displacement of the ligand atoms from the least-squares plane for the complexes. Both copper and nickel complexes are closer to planarity than the zinc complex. Complexes **1** and **4**, which show the same behaviour of the ligand, show a similar pattern, although in the nickel complex both sulfur atoms show identical deviation with respect to the least-squares plane, which agrees with the minimum degree of deviation from planarity in this complex, probably due to the better fit of the nickel atom. Moreover, the deviation from planarity of complexes **2** and **3** shows the same pattern, namely two distances for the sulfur and the imine nitrogen atoms, which agrees with the asymmetry in the ligand and the tetragonal deformation in the metal environment. Additional information can be gained from the torsion angles: the value of the N(3)–C(2)–C(3)–N(4) torsion angle is less than 2° for the complexes, except for the zinc complex, where it is 4.1°.

The presence of terminal nitrogen atoms gives rise to intermolecular N–H–N hydrogen bonds, which lead to extended architectures in all complexes. The intermolecular contact distances are listed in Table 3. Complex **1** shows intermolecular interactions between the terminal amine group and the deprotonated secondary amine, as was shown in complex **4**, although N–H–S hydrogen bonds do

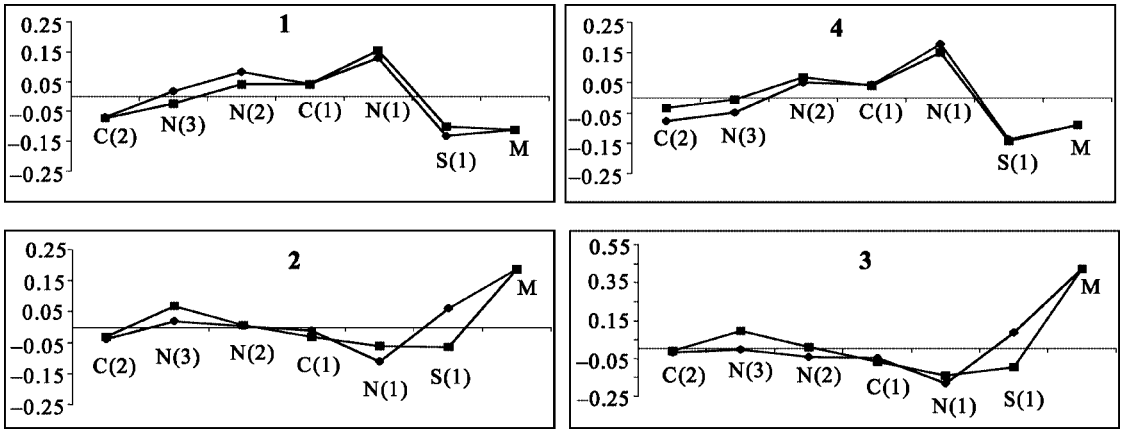

Figure 8. Displacement of atoms [Å] from least-squares plane defined by C(1), C(2), C(3), C(4), N(1), N(2), N(3), N(4), N(5), N(6), S(1), S(2) and M.

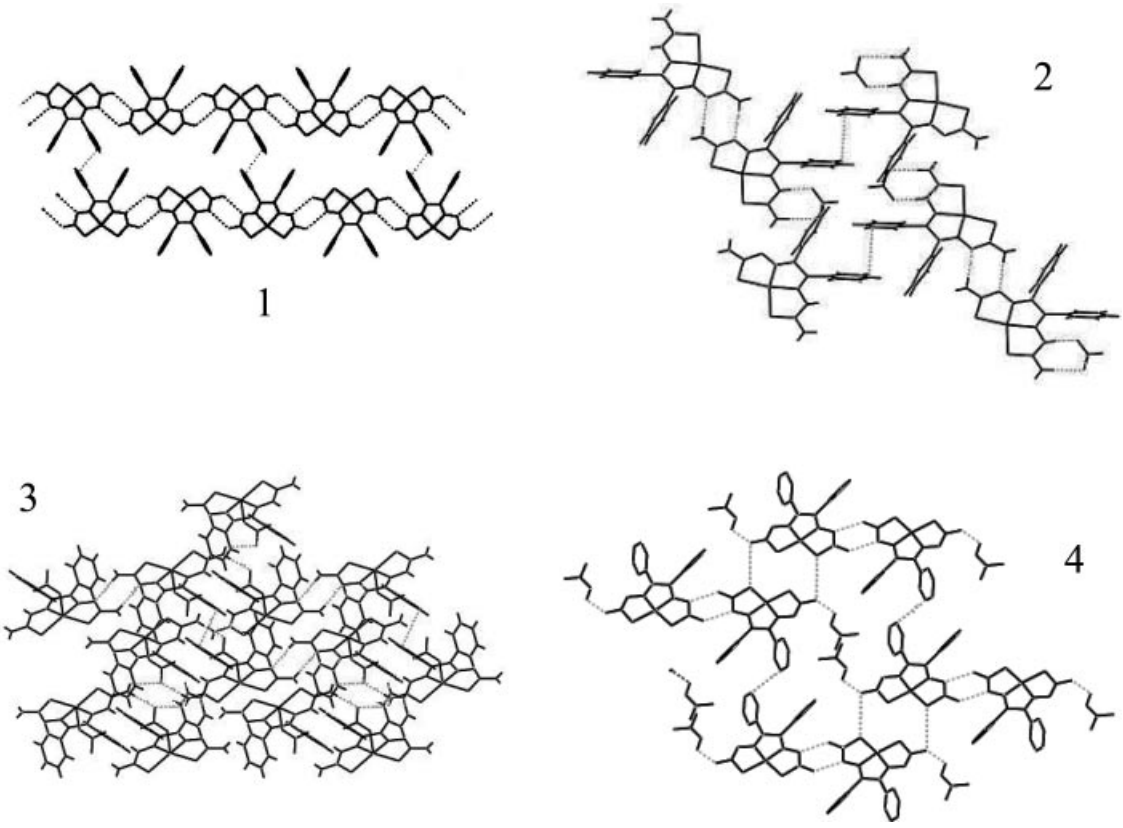

Figure 9. N–H–N hydrogen bonds and π–π interactions in the complexes.

not appear in the free ligand or in complex **4**.[27] Complex **1** is formed by flat ribbons that are linked through π–π interactions between the phenyl rings, which are at 3.644 Å (Figure 9). In complexes **2** and **3**, the molecules are linked to form couples by paired N(1)–H(1B)–N(2) hydrogen bonds, and these couples are linked by π–π interactions between the phenyl rings at 3.459 and 3.401 Å, respectively. They also contain hydrogen bonds to the nitrate ions, although in a different way: Complex **2** contains interactions between two oxygen atoms and both primary and secondary amine groups from the neutral thiosemicarbazone branch, whereas in complex **3** the nitrate group interacts also with NH and NH_2 groups, but belonging to two different chains, instead of to the same thiosemicarbazone arm (Figure 9). Complex **4** shows an intermolecular structure similar to those of complex **2**, but with hydrogen bonds with the DMF molecule. Couples are linked by π–π interactions with a distance of 3.376 Å.

Conclusions

The copper complexes are inherently planar and the zinc complex shows a distorted square-based pyramidal geometry with the nitrate group in the apical position, as proposed from the spectroscopic data. The bond length and angles for the complexes agree with the variable grade of deprotonation in the ligand and the requirements of the metal ion. The complexes present a variable grade of distortion from planarity although they all present intermolecular interactions, especially pairs of N(1)–H(1B)–N(2) hydrogen bonds and π–π interactions between the phenyl rings. Complex **1** shows the smallest deviation with respect to the planar nickel complex **4**. The presence of a hydrazinic hydrogen and a nitrate group in complexes **2** and **3** changes the intermolecular interactions, which increases the deviation from planarity, as reflected in the reduction potential of complex **2**. We have established the relationship between the distorted geometry and the reduction potential of copper complexes. In complex **1**, this parameter is close to those of copper bis(thiosemicarbazones) with hypoxic selectivity, therefore some activity could be expected.

Experimental Section

Physical Measurements: Microanalyses were carried out with a Perkin–Elmer 2400 II CHNS/O Elemental Analyser. IR spectra in the 4000–400 cm^{-1} range were recorded as KBr pellets on a Jasco FT/IR-410 spectrophotometer. FAB mass spectra were recorded on a VG Auto Spec instrument using Cs as the fast atom and *m*-nitrobenzyl alcohol (*m*-NBA) as the matrix. Conductivity data were measured for freshly prepared DMF solutions (ca. 10^{-3} M) at 25 °C with a Metrohm Herisau model E-518 instrument.

Synthesis: Thiosemicarbazide (Fluka), benzil (Aldrich), copper(II) nitrate trihydrate (Merck), copper(II) chloride dihydrate (Aldrich) and zinc(II) nitrate hexahydrate (Fluka) were used as received.

Benzil Bis(thiosemicarbazone) (LH_6): This compound was prepared following the procedure reported previously.[37] FAB-MS (*m*-NBA):

m/z (%) = 357 (25) $[M + 1]^+$. IR (KBr): $\tilde{\nu}$ = 3420, 3386, 3342, 3330, 3210, 3151 (NH); 1608 (NH_2); 1581 (C=N); 848 (CS) cm^{-1}.

[$CuLH_4$] (1):[26] A solution of copper(II) chloride dihydrate (120 mg, 0.70 mmol) in methanol (20 mL) was added to a suspension of LH_6 (500 mg, 1.40 mmol) in methanol (20 mL). The mixture was stirred for 48 h at room temperature. The reddish solid formed was filtered off, washed with methanol and dried in vacuo (yield: 65 mg, 22%). FAB-MS (*m*-NBA): *m/z* (%) = 418 (30) $[M + 1]^+$. IR (KBr): $\tilde{\nu}$ = 3343, 3271, 3102 (NH) + (NH_2); 1626, 1600, 1569 (C=N) + (NH_2); 1467, 1427 thioamide II; 836 thioamide IV; 449 (Cu–N); 428 (Cu–S) cm^{-1}. Recrystallisation from DMSO gave reddish crystals suitable for X-ray analysis.

[$CuLH_5$]NO_3 (2): A solution of copper(II) nitrate trihydrate (360 mg, 1.49 mmol) in methanol (20 mL) was added to a suspension of LH_6 (500 mg, 1.40 mmol) in methanol (20 mL). The mixture was stirred for 19 h at room temperature. The brown solid formed was filtered off, washed with methanol and dried in vacuo.[26] A black solid (**2**) was isolated from the mother liquor. $C_{16}H_{15}CuN_7S_2O_3$ (480.55): calcd. C 39.95, H 3.12, N 20.39, S 13.31; found C 39.63, H 2.98, N 20.77, S 13.02. FAB-MS (*m*-NBA): *m/z* (%) = 418 (50) $[M - NO_3]^+$. IR (KBr): $\tilde{\nu}$ = 3443, 3408, 3274, 3097 (NH) + (NH_2); 1663, 1628, 1604 (C=N) + (NH_2); 1554, 1534, 1490, 1444 thioamide II; 778 thioamide IV; 475 (Cu–N); 428 (Cu–S) cm^{-1}. Λ_M = 86 $\Omega^{-1}cm^2mol^{-1}$. Black crystals suitable for X-ray analysis were obtained from the mother liquor after a week in the freezer.

[$ZnLH_5NO_3$] (3):[28] A solution of zinc(II) nitrate hexahydrate (520 mg, 1.75 mmol) in ethanol (10 mL) was added to a suspension of LH_6 (500 mg, 1.40 mmol) in ethanol (40 mL). The mixture was stirred under reflux for 4 h. The yellow-orange solid was filtered off, washed with ethanol and dried in vacuo (yield: 305 mg, 45%). FAB-MS (*m*-NBA): *m/z* (%) = 419 (100) $[M - NO_3]^+$. IR (KBr): $\tilde{\nu}$ = 3440, 3268, 3111 (NH); 3421, 3169 $\nu(NH_2)$; 1629, 1576 (C=N); 1615 (NH_2); 1439 thioamide II; 816 thioamide IV; 447 (Zn–N); 341 (Zn–S) cm^{-1}. Λ_M = 51 $\Omega^{-1}cm^2mol^{-1}$. Yellow crystals suitable for X-ray analysis were obtained by recrystallisation from methanol.

[$NiLH_4$] (4): This compound was prepared following the procedure previously described.[27]

Crystallography: Single crystals of complexes **1** and **3** were obtained by recrystallisation from DMSO and methanol, respectively, and crystals of **2** were isolated from the mother liquor of the reaction. Crystals of the compounds were mounted on a glass fibre and transferred to a Bruker SMART 6 K CCD area-detector three-circle diffractometer with a MAC Science Co., Ltd. Rotating Anode generator (Cu-K_α radiation, λ = 1.54178 Å) equipped with Goebel mirrors at settings of 50 kV and 110 mA. X-ray data were collected with a combination of six runs at different φ and 2θ angles for 3600 frames. The substantial redundancy in data allows empirical absorption corrections (SADABS)[32] to be applied using multiple measurements of symmetry-equivalent reflections (ratio of minimum to maximum apparent transmission: 0.578995 for complex **1**, 0.514195 for complex **2** and 0.722376 for complex **3**). The unit cell parameters were obtained by full-matrix least-squares refinements of 4562 reflections for complex **1**, 4593 reflections for complex **2** and 4356 reflections for complex **3**. Crystallographic details are reported in Table 4. The raw intensity data frames were integrated with the SAINT[33] program, which was also used to apply corrections for Lorentz and polarisation effects.

The software package SHELXTL[34] version 6.10 was used for space group determination, structure solution and refinement. The structures were solved by direct methods (SHELXS-97),[35] completed with difference Fourier syntheses, and refined with full-matrix least-squares using SHELXL-97[36] by minimizing $\omega(F_o^2 - F_c^2)^2$. Weighted *R* factors (R_w) and all goodness-of-fit (*S*) values are based on F^2; conventional *R* factors (*R*) are based on *F*. All non-hydrogen atoms were refined with anisotropic displacement parameters. All scattering factors and anomalous dispersions factors are contained in the SHELXTL 6.10 program library. The high quality of the data set allowed all hydrogen atoms to be located by difference maps and refined isotropically in all complexes.
CCDC-258838 (for **1**), -258839 (for **2**) and -258840 (for **3**) contain the supplementary crystallographic data for this paper. These data

Table 4. Crystal data and structure refinement for complexes **1**, **2** and **3**.

	1	**2**	**3**
Formula	$C_{16}H_{14}CuN_6S_2$	$C_{16}H_{15}CuN_7O_3S_2$	$C_{16}H_{15}N_7O_3S_2Zn$
Formula mass	417.99	481.01	482.84
Temperature [K]	296	100	293
Crystal system	triclinic	triclinic	triclinic
Space group	$P\bar{1}$	$P\bar{1}$	$P\bar{1}$
a [Å]	8.9504(10)	7.9999(10)	7.9889(10)
b [Å]	9.5991(10)	10.6314(10)	10.7110(13)
c [Å]	10.8885(10)	12.3778(2)	12.4027(17)
α [°]	99.456(10)	86.162(10)	85.859(8)
β [°]	106.114(10)	77.177(10)	75.065(9)
γ [°]	92.456(10)	68.452(10)	68.518(8)
Volume [Å^3]	882.66(16)	954.69(2)	953.9(2)
Z	2	2	2
Density (calcd.) [Mg m^{-3}]	1.573	1.673	1.681
Absorption coefficient	4.055 mm^{-1}	3.976 mm^{-1}	4.152 mm^{-1}
F(000)	426	490	492
Goodness of fit on F^2	1.076	1.038	1.029
Reflection collected	7179	7352	7141
Independent reflections	2613	3277	3261
Final *R* indices	R_1 = 0.0345	R_1 = 0.0294	R_1 = 0.0339
[$I > 2\sigma(I)$]	wR_2 = 0.0967	wR_2 = 0.0797	wR_2 = 0.0899
R indices (all data)	R_1 = 0.0385, wR_2 = 0.0999	R_1 = 0.312, wR_2 = 0.0809	R_1 = 0.0369, wR_2 = 0.0926

can be obtained free of charge from The Cambridge Crystallographic Data Centre via www.ccdc.cam.ac.uk/data_request/cif.

Acknowledgments

We thank the DGICYT for financial support (project BQU2001-0151).

[1] D. X. West, S. B. Padhye, P. B. Sonawane, *Struct. Bond. (Berlin)* **1991**, *76*, 1–50.
[2] A. E. Liberta, D. X. West, *Biometals* **1992**, *5*, 121–126.
[3] *International Encyclopaedia of Pharmacology and Therapeutics* (Eds.: J. G. Cory, A. H. Cory), Pergamon Press, New York, **1989**.
[4] J. Easmon, G. Purstinger, G. Heinish, T. Roth, H. H. Fiebig, W. Holzer, W. Jager, M. Jenny, J. Hofman, *J. Med. Chem.* **2001**, *44*, 2164–2171.
[5] D. H. Petering, *Bioinorg. Chem.* **1972**, *1*, 255–271.
[6] D. X. West, A. E. Liberta, S. B. Padhye, R. C. Chikate, P. B. Sonawane, A. S. Kumbhar, R. G. Yeranda, *Coord. Chem. Rev.* **1993**, *123*, 49–71 and references cited therein.
[7] C. M. Liu, G. Xiong, X. Z. You, Y. J. Liu, *Polyhedron* **1996**, *15*, 4565–4571.
[8] P. J. Blower, T. C. Castle, A. R. Cowley, J. R. Dilworth, P. S. Donnelly, E. Labisbal, F. E. Sowrey, S. J. Teat, M. J. Went, *Dalton Trans.* **2003**, 4416–4425.
[9] Y. Fujibayashi, H. Taniuchi, Y. Yonekura, H. Ohtani, J. Konishi, A. Yokoyama, *J. Nucl. Med.* **1997**, *38*, 1155–1160.
[10] H. Okazawa, Y. Yonekura, Y. Fujibayashi, S. Nishizawa, Y. Magata, K. Ishizu, F. Tanaka, T. Tsuchida, N. Tamaki, J. Konishi, *J. Nucl. Med.* **1994**, *35*, 1910–1915.
[11] J. S. Lewis, J. M. Connett, J. R. Garbow, T. L. Buettner, Y. Fujibayashi, J. W. Fleshman, M. J. Welch, *Cancer Res.* **2002**, *62*, 442–449.
[12] A. Obata, S. Kasamatsu, J. S. Lewis, T. Furucawa, S. Takamatsu, J. Toyohara, T. Asai, M. J. Welch, S. G. Adams, H. Saji, Y. Yonekura, Y. Fujibayashi, *Nucl. Med. Biol.* **2005**, *32*, 21–28.
[13] J. L. J. Dearling, J. S. Lewis, D. W. McCarthy, M. J. Welch, P. J. Blower, *Chem. Commun.* **1998**, 2531–2532.
[14] J. L. J. Dearling, J. S. Lewis, G. D. Mullen, M. J. Welch, P. J. Blower, *J. Biol. Inorg. Chem.* **2002**, *7*, 249–259.
[15] A. R. Cowley, J. R. Dilworth, P. S. Donnelly, E. Labisbal, A. Sousa, *J. Am. Chem. Soc.* **2002**, *124*, 5270–5271.
[16] G. J. Mathias, M. J. Welch, D. J. Perry, A. H. McGuire, X. Zhu, J. M. Connett, M. A. Green, *Nucl. Med. Biol.* **1991**, *18*, 807–811.
[17] P. Herrero, J. J. Hartman, M. A. Green, C. J. Anderson, M. J. Welch, J. Markham, S. R. Bergmann, *J. Nucl. Med.* **1996**, *37*, 1294–1300.
[18] E. K. John, M. A. Green, *J. Med. Chem.* **1990**, *33*, 1764–1770.
[19] M. A. Green, *Transition Met. Chem.* **1997**, *22*, 427–429.
[20] L. J. Ackerman, P. E. Fanwick, M. A. Green, E. John, W. E. Running, J. K. Swearingen, J. W. Webb, D. X. West, *Polyhedron* **1999**, *18*, 2759–2767.
[21] J. L. J. Dearling, J. S. Lewis, G. D. Mullen, M. T. Rae, J. Zweit, P. J. Blower, *Eur. J. Nucl. Med.* **1998**, *25*, 788–792.
[22] C. J. Anderson, M. J. Welch, *Chem. Rev.* **1999**, *99*, 2219–2234.
[23] R. I. Maurer, J. P. Blower, J. R. Dilworth, C. D. Reynolds, Y. Zheng, G. D. Mullen, *J. Med. Chem.* **2002**, *45*, 1420–1431.
[24] H. Beraldo, D. Gambino, *Mini-Rev. Med. Chem.* **2004**, *4*, 31–39.
[25] A. R. Cowley, J. Davis, J. R. Dilworth, P. S. Donnelly, R. Dobson, A. Nightingale, J. M. Peach, D. Kerr, L. Seymur, *Chem. Commun.* **2005**, 845–847.
[26] E. Franco, E. López-Torres, M. A. Mendiola, M. T. Sevilla, *Polyhedron* **2000**, *19*, 441–451.
[27] E. López-Torres, M. A. Mendiola, C. J. Pastor, B. Souto Pérez, *Inorg. Chem.* **2004**, *43*, 5222–5230.
[28] E. López-Torres, M. A. Mendiola, J. Rodríguez-Procopio, M. T. Sevilla, E. Colacio, J. M. Moreno, I. Sobrados, *Inorg. Chim. Acta* **2001**, *323*, 130–138.
[29] a) G. W. Bushnell, A. Y. M. Tsang, *Can. J. Chem.* **1979**, *57*, 603–607; b) Y. Xinkan, W. Honggen, W. Ruji, H. Ling, W. Genglin, *Gaodeng Xuexiao Huaxue Xuebao* **1988**, *9*, 484–487.
[30] A. W. Addison, T. N. Rao, J. Reedijk, J. van Rijnand, G. C. Verschoor, *J. Chem. Soc., Dalton Trans.* **1984**, 1349–1356.
[31] H. Yokoi, A. W. Addison, *Inorg. Chem.* **1977**, *16*, 1341–1349.
[32] G. M. Sheldrick, SADABS version 2.03, *Program for Empirical Absorption Correction*, University of Göttingen, **1997**–**2001**.
[33] G. M. Sheldrick, *SAINT+NT* (version 6.04) *SAX Area-Detector Integration Program*, Bruker AXS, Madison, WI, **1997**–**2001**.
[34] Bruker AXS SHELXTL (version 6.10,) Structure Determination Package, Bruker AXS, Madison, WI, **2000**.
[35] SHELXS-97, *Program for Structure Solution*: G. M. Sheldrick, *Acta Crystallogr., Sect. A* **1990**, *46*, 467–473.
[36] G. M. Sheldrick, SHELXL-97, *Program for Crystal Structure Refinement*, University of Göttingen, **1997**.
[37] P. Souza, M. A. Mendiola, A. Arquero, V. Fernández, E. Gutiérrez-Puebla, C. Ruíz-Valero, *Z. Naturforsch. Teil B* **1994**, *49*, 263–271.

Received: April 25, 2005
Published Online: September 19, 2005

